Euclidean random matrix theory: low-frequency non-analyticities and Rayleigh scattering

Carl Ganter, Walter Schirmacher

Euclidean random matrix theory: low-frequency non-analyticities and Rayleigh scattering

Journal:	*Philosophical Magazine & Philosophical Magazine Letters*
Manuscript ID:	TPHM-10-Jun-0291.R1
Journal Selection:	Philosophical Magazine
Date Submitted by the Author:	12-Sep-2010
Complete List of Authors:	Ganter, Carl; Technische Universität München, Institut für Radiologie Schirmacher, Walter; Universität Mainz, Institut für Physik
Keywords:	theoretical, disorder, phonons, hopping transport, diffusion
Keywords (user supplied):	Rayleigh scattering

Philosophical Magazine
Vol. 00, No. 00, 00 Month 200x, 1–17

RESEARCH ARTICLE

Euclidean random matrix theory: low-frequency non-analyticities and Rayleigh scattering

Carl Ganter[a] and Walter Schirmacher[b*]

[a] *Institut für Röntgendiagnostik, Technische Universität München, Ismaninger Str. 22, D-81675 München, Germany* ; [b] *Institut für Physik, Universität Mainz, D-55099 Mainz, Germany*

(*Received 00 Month 200x; final version received 00 Month 200x*)

By calculating all terms of the high-density expansion of the euclidean random matrix theory (up to second-order in the inverse density) for the vibrational spectrum of a topologically disordered system we show that the low-frequency behavior of the self energy is given by $\Sigma(k,z) \propto k^2 z^{d/2}$ and not $\Sigma(k,z) \propto k^2 z^{(d-2)/2}$, as claimed previously. This implies the presence of Rayleigh scattering and long-time tails of the velocity autocorrelation function of the analogous diffusion problem of the form $Z(t) \propto t^{(d+2)/2}$.

Keywords: topolocigal disorder; euclidean random matrix; Rayleigh scattering; diffusion; long-time tails; velocity autocorrelation function; low-frequency nonanalyticity

1. Introduction

Rayleigh scattering [1], i.e. the fact that the mean-free path of weakly scattered waves varies as $\omega^{-(d+1)}$ in a d-dimensional disordered medium as $\omega \to 0$, is widely believed to be a general property of quenched disordered matter [2–6]. However, **R.1** recently it has been claimed [7] that a harmonic system with displacements $u_i(t)$ obeying

$$\frac{\mathrm{d}^2}{\mathrm{d}t^2} u_i(t) = -\sum_j t_{ij}\big(u_i(t) - u_j(t)\big)\,, \tag{1}$$

where i and j denote random sites $\mathbf{r}_{i,j}$ in d-dimensional space, would have wave-like excitations, which have a line-width (inverse mean-free path), varying with ω^2 instead of ω^4 in $d = 3$. t_{ij} are force constants, divided the mass at the node i, which are assumed to depend on the distance, i.e. $t_{ij} = t(r_{ij})$. The claim of absence of Rayleigh scattering had been substantiated by a high-density expansion and a diagrammatical analysis [7]. This claim is not only astonishing with respect to the mentioned general view on waves in disordered media, but it is also in contradiction with the known analytic properties of the analogous diffusion system. If one replaces the double time derivative in (1) by a single one, one obtains the

*Corresponding author. Email: walter.schirmacher@ph.tum.de

ISSN: 1478-6435 print/ISSN 1478-6443 online

DOI: 10.1080/14786435.20xx.xxxxxx
http://www.informaworld.com

equation of a random walk among the sites i, j:

$$\frac{\mathrm{d}}{\mathrm{d}t} n_i(t) = -\sum_j t_{ij}\big(n_i(t) - n_j(t)\big)\,, \tag{2}$$

where $n_i(t)$ give the odds for the walker to be at i at time t and $t_{ij} = t(r_{ij})$ is the hopping probability per unit time. Eq. (2) describes e.g. the motion of electrons hopping among shallow impurities in a semiconductor [8, 9, 11, 12]. Such a random walk is known [10] to exhibit a long-time tail of the velocity-autocorrelation function (VAF) varying as $Z(t) \propto t^{(d+2)/2}$ for $t \to \infty$ [10, 13], a feature shared with Lorentz models [13–15]. In fact, the Laplace transform of the VAF is the frequency-dependent diffusivity $D(z = i\omega + \epsilon)$, which has, according to the Tauberian theorems [16] a low-frequency singularity $D(z) \to z^{d/2}, |z| \to 0$. Now, in the analogous vibrational problem this quantity corresponds to the square of a frequency-dependent sound velocity $D(z = -\omega^2 + i\epsilon) = v^2(z)$. The imaginary part $v''(\omega)$ of the latter is related to the mean-free path via

$$\frac{1}{\ell(\omega)} = \frac{2\omega v''(\omega)}{|v(z)|^2} \tag{3}$$

This gives $\ell \propto \omega^{-(d+1)}$, i.e. Rayleigh scattering. We conclude that the long-time tail of the VAF in the diffusion problem is mathematically equivalent to the Rayleigh-scattering property.

In the following we calculate all irreducible diagrams (self-energy diagrams) up to second order in the inverse density $\rho^{-1} = V/N$, where N is the number of sites and V the volume. We show that to this order the self energy is proportional to $k^2 z^{d/2}$, $z = i\omega + \epsilon$ (diffusion) or $z = -\omega^2 + i\epsilon$ (sound). and not as claimed in Refs. [7] $\propto k^2 z^{(d-2)/2}$. We also show, why the so-called cactus approximation for a self-consistent theory erroneously leads to a non-analyticity $z^{(d-2)/2}$ instead of $z^{d/2}$.

2. Formalism

As in refs. [7] we start from a high-frequency (z) and high-density ($\rho = N/V$) expansion of the averaged propagator

$$G(\mathbf{k}, z) = \frac{1}{N}\sum_{mn}\left\langle e^{i\mathbf{k}\mathbf{r}_{mn}}[z\mathbf{1} - \mathbf{M}]^{-1}_{mn}\right\rangle = \frac{1}{z}$$
$$+\sum_{p=1}^{\infty}\frac{1}{z^{p+1}}\frac{1}{N}\sum_{i_0\ldots i_p}\left\langle e^{i\mathbf{k}\mathbf{r}_{i_0 i_1}}M_{i_0 i_1}\ldots e^{i\mathbf{k}\mathbf{r}_{i_{p-1} i_p}}M_{i_{p-1} i_p}\right\rangle$$

Here $\mathbf{M}$ is a matrix with off-diagonal elements $M_{ij} = t_{ij}$ and diagonal elements $M_{ii} = -\sum_{\ell\neq i} t_{i\ell}$. $t(k) = t(\mathbf{k})$ is the d-dimensional Fourier transform of $t(r)$.

The configurationally averaged Green's function can now be expressed in terms of the irreducible self energy $\Sigma(k, z)$ as follows

$$G(k, z) = \frac{1}{z - \rho\,[\,t(k) - t(0)\,] - \Sigma(k, z)} \overset{k\to 0}{=} \frac{1}{z + D(z)k^2} \tag{4}$$

The frequency-dependent diffusivity/sound velocity is given by

$$D(z) = v(z)^2 = -\frac{1}{2}\frac{\partial^2}{\partial k^2}\Big[t(k) + \Sigma(k,z)\Big]_{k\to 0} \tag{5}$$

For simplicity, we assume complete site disorder (i.e. the radial pair correlation function $g(r) \equiv 1$). Therefore $t(k)$ is simply the Fourier transform of the transition rate $t(r)$ [17].

It is possible, to consider a more general case, e.g. by replacing $t^n(r_{ij}) \to g(r_{ij})\, t^n(r_{ij})$ $(n > 0)$ in every diagram (Kirkwood factorization). Without proof, it can be demonstrated that the analytical properties of the first and second order diagrams would remain unaffected by such an extension. **R.4**

We denote the unrenormalized part of the Green's function by G_0:

$$G_0(k,z) := \frac{1}{z - \rho\,[\,t(k) - t(0)\,]} \tag{6}$$

In analogy to the approach in Ref. [7], it is helpful to consider a high-density expansion of the propagator, which is in turn determined by an analogous expansion the self energy $\Sigma(k,z)$

$$\Sigma(k,z) =: \sum_{n=1}^{\infty} \rho^{-n}\, \Sigma^{(n)}(k,z)\,, \tag{7}$$

As outlined in [7], the index n counts repetitions of sites in the high frequency / high density expansion.

In the following, we will derive exact results for $n = 1$ and $n = 2$.

To this end, we will use diagrammatic representations (as explained in Figure 1), to distinguish topologically different contributions to the self energy.

In the following, we calculated the diagrams for the special case $d = 3$, but the results remain valid for arbitrary dimensions. **R.3**

3. First-order diagrams: $\boldsymbol{\Sigma^{(1)}(k,z)}$

This case is comparably trivial and requires the addition of four diagrams (cf. Figure 1), since the first and last connection can refer to an off–diagonal (**O**) or a diagonal (**D**) transition rate.

$$\mathbf{OO} = \rho \int \frac{d\mathbf{p}}{(2\pi)^3}\, t^2(p)\; G_0(p,z)$$

$$\mathbf{OD} = -\,\rho \int \frac{d\mathbf{p}}{(2\pi)^3}\, t(\mathbf{k}-\mathbf{p})\; t(p)\; G_0(p,z)$$

$$\mathbf{DO} = -\,\rho \int \frac{d\mathbf{p}}{(2\pi)^3}\, t(\mathbf{k}-\mathbf{p})\; t(p)\; G_0(p,z)$$

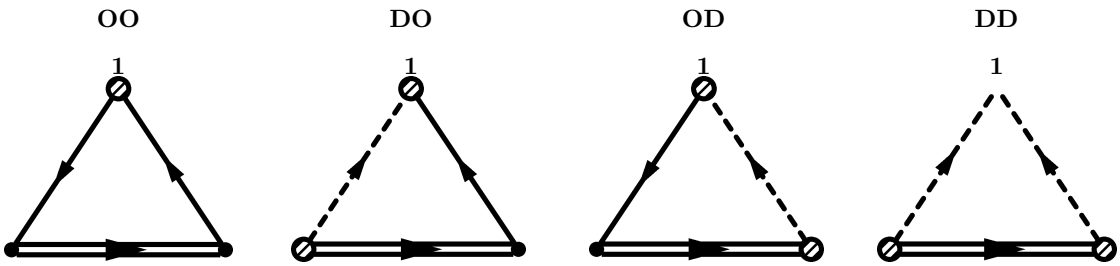

Figure 1. Irreducible diagrams in $\Sigma^{(1)}(k,z)$.
Off-diagonal matrix elements, $t^o_{ij} \equiv t(r_{ij})$, associated with a site change, are represented by solid lines. Dashed lines do not effect a site change. The associated transition rates $t^d_{ij} \equiv -t(r_{ij})$ belong to the diagonal matrix elements and are a consequence of the sum rule.
The unrenormalized propagator $[G_0]_{ij} \equiv G_0(r_{ij})$ is shown as a double-line. Note that the propagator contains a diagonal part (for $i=j$ the diagram has length zero) $\mathcal{G}_0(z) := [z + \rho\, t(0)]^{-1}$, which is formally obtained as $\mathcal{G}_0(z) = \lim_{k\to\infty} G_0(k,z)$. In most cases, this requires no special attention. Exceptions, when these terms need to be explicitly excluded to preserve irreducibility will be mentioned below.
Open circles will always indicate start and end points of a diagram.

$$\mathbf{DD} = \rho \int \frac{d\mathbf{p}}{(2\pi)^3}\, t^2(\mathbf{k}-\mathbf{p})\; G_0(p,z)$$

Added together:

$$\rho \int \frac{d\mathbf{p}}{(2\pi)^3} \left[\, t(\mathbf{k}-\mathbf{p}) - t(p) \,\right]^2 G_0(p,z) \tag{8}$$

Since we are mainly interested in the imaginary part of

$$\lim_{z\to 0} \lim_{k\to 0} \Sigma(k,z) \tag{9}$$

we will have to examine the bracket in Eq. (8) in the limit $k \to 0$

$$\lim_{k\to 0}\, t(\mathbf{k}-\mathbf{p}) - t(p) = \frac{t'(p)}{p}\cdot\mathbf{kp} + \frac{1}{2}\,\frac{t''(p)\cdot p - t'(p)}{p^3}\cdot[\,\mathbf{kp}\,]^2 + \frac{1}{2}\,\frac{t'(p)}{p}\cdot k^2 + \mathcal{O}\left(k^3\right) \tag{10}$$

We therefore obtain

$$\lim_{p\to 0} \lim_{k\to 0} \left[\, t(\mathbf{k}-\mathbf{p}) - t(p) \,\right]^2 = c\cdot \underbrace{[\,\mathbf{kp}\,]^2}_{\propto p^2} + \mathcal{O}\left(k^3,\, p^3\right) \tag{11}$$

with some usually nonzero constant c. With the additional p^2 factor from the threedimensional integral, we obtain from the diffusion pole of $G_0(k,z)$

$$\lim_{z\to 0} \lim_{k\to 0} \mathrm{Im}\left[\, \Sigma^{(1)}(k,z) \,\right] \propto z^{3/2} k^2 \tag{12}$$

4. Second-order diagrams: $\Sigma^{(2)}(k,z)$

This case is considerably more complex. It turns out to be advantegeous to consider topologically different groups of irreducible diagrams separately:

- $\Sigma^{(2)}_{\alpha}(k,z)$: $(1*2\cdots2\cdots1)$
- $\Sigma^{(2)}_{\beta}(k,z)$: $(1\,2\cdots2\cdots1)$
- $\Sigma^{(2)}_{\gamma}(k,z)$: $(1*2\cdots1\cdots2)$
- $\Sigma^{(2)}_{\delta}(k,z)$: $(1\,2\cdots1\cdots2)$
- $\Sigma^{(2)}_{\varepsilon}(k,z)$: $(1\cdots1\cdots1)$

Unlike in $\cdots$ at least one additional site index (differnt from 1 and 2) needs to be contained in $*$.

The complete and exact second-order self energy is then just the sum of these partial contributions:

$$\Sigma^{(2)}(k,z) = \Sigma^{(2)}_{\alpha}(k,z) + \Sigma^{(2)}_{\beta}(k,z) + \Sigma^{(2)}_{\gamma}(k,z) + \Sigma^{(2)}_{\delta}(k,z) + \Sigma^{(2)}_{\varepsilon}(k,z) \qquad (13)$$

4.1. $\Sigma^{(2)}_{\alpha}(k,z)$: *Irreducible Diagrams* $(1*2\cdots2\cdots1)$

Here, the 16 diagrams in Figure 2 need to be distinguished [18]:

$$\mathbf{OOOO} = \rho^2 \int d\mathbf{p}\, d\mathbf{q}\; t^3(p)\; t(q)\; G_0^2(p)\; G_0(q)$$

$$\mathbf{OOOD} = -\rho^2 \int d\mathbf{p}\, d\mathbf{q}\; t(\mathbf{k}-\mathbf{p})\; t^2(p)\; t(q)\; G_0^2(p)\; G_0(q)$$

$$\mathbf{OODO} = -\rho^2 \int d\mathbf{p}\, d\mathbf{q}\; t^3(p)\; t(\mathbf{p}-\mathbf{q})\; G_0^2(p)\; G_0(q)$$

$$\mathbf{OODD} = \rho^2 \int d\mathbf{p}\, d\mathbf{q}\; t(\mathbf{k}-\mathbf{p})\; t^2(p)\; t(\mathbf{p}-\mathbf{q})\; G_0^2(p)\; G_0(q)$$

$$\mathbf{ODOO} = -\rho^2 \int d\mathbf{p}\, d\mathbf{q}\; t^2(p)\; t(\mathbf{p}-\mathbf{q})\; t(q)\; G_0^2(p)\; G_0(q)$$

$$\mathbf{ODOD} = \rho^2 \int d\mathbf{p}\, d\mathbf{q}\; t(\mathbf{k}-\mathbf{p})\; t(p)\; t(\mathbf{p}-\mathbf{q})\; t(q)\; G_0^2(p)\; G_0(q)$$

$$\mathbf{ODDO} = \rho^2 \int d\mathbf{p}\, d\mathbf{q}\; t^2(p)\; t^2(\mathbf{p}-\mathbf{q})\; G_0^2(p)\; G_0(q)$$

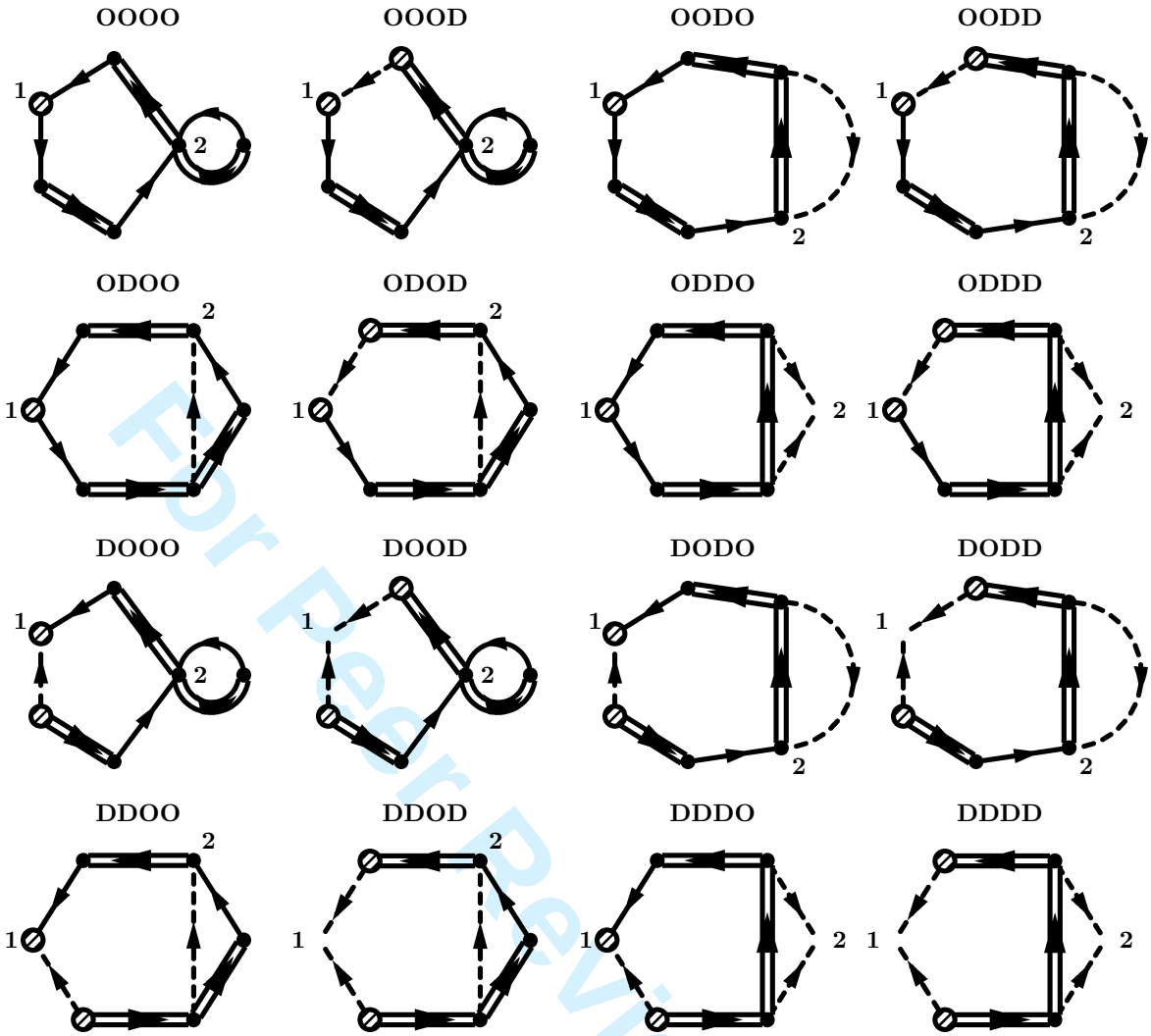

Figure 2. Irreducible Diagrams in $\Sigma_{\alpha}^{(2)}(k,z)$

$$\mathbf{ODDD} = -\rho^2 \int d\mathbf{p}\, d\mathbf{q}\; t(\mathbf{k}-\mathbf{p})\; t(p)\; t^2(\mathbf{p}-\mathbf{q})\; G_0^2(p)\; G_0(q)$$

$$\mathbf{DOOO} = -\rho^2 \int d\mathbf{p}\, d\mathbf{q}\; t(\mathbf{k}-\mathbf{p})\; t^2(p)\; t(q)\; G_0^2(p)\; G_0(q)$$

$$\mathbf{DOOD} = \rho^2 \int d\mathbf{p}\, d\mathbf{q}\; t^2(\mathbf{k}-\mathbf{p})\; t(p)\; t(q)\; G_0^2(p)\; G_0(q)$$

$$\mathbf{DODO} = \rho^2 \int d\mathbf{p}\, d\mathbf{q}\; t(\mathbf{k}-\mathbf{p})\; t^2(p)\; t(\mathbf{p}-\mathbf{q})\; G_0^2(p)\; G_0(q)$$

$$\mathbf{DODD} = -\rho^2 \int d\mathbf{p}\, d\mathbf{q}\; t^2(\mathbf{k}-\mathbf{p})\; t(p)\; t(\mathbf{p}-\mathbf{q})\; G_0^2(p)\; G_0(q)$$

$$\mathbf{DDOO} = \rho^2 \int d\mathbf{p}\, d\mathbf{q}\; t(\mathbf{k}-\mathbf{p})\; t(p)\; t(\mathbf{p}-\mathbf{q})\; t(q)\; G_0^2(p)\; G_0(q)$$

$$\mathbf{DDOD} = -\rho^2 \int d\mathbf{p}\, d\mathbf{q}\; t^2(\mathbf{k}-\mathbf{p})\; t(\mathbf{p}-\mathbf{q})\; t(q)\; G_0^2(p)\; G_0(q)$$

$$\mathbf{DDDO} = -\rho^2 \int d\mathbf{p}\, d\mathbf{q}\; t(\mathbf{k}-\mathbf{p})\; t(p)\; t^2(\mathbf{p}-\mathbf{q})\; G_0^2(p)\; G_0(q)$$

$$\mathbf{DDDD} = \rho^2 \int d\mathbf{p}\, d\mathbf{q}\; t^2(\mathbf{k}-\mathbf{p})\; t^2(\mathbf{p}-\mathbf{q})\; G_0^2(p)\; G_0(q)$$

Added together:

$$\Sigma_\alpha^{(2)}(k,z) = \tag{14}$$
$$\rho^2 \int d\mathbf{p}\, d\mathbf{q}\; [\,t(\mathbf{k}-\mathbf{p}) - t(p)\,]^2\; [\,t(\mathbf{p}-\mathbf{q}) - t(p)\,]\; [\,t(\mathbf{p}-\mathbf{q}) - t(q)\,]\; G_0^2(p)\; G_0(q)$$

Two cases need to be distinguished:

p is small: Because of Eq. (11), the first squared bracket delivers a factor p^2. Additional p^2 factors result from the third bracket and the 3D integration, respectively, so that we finally arrive at a p^6 factor. From the identity $G_0^2(p,z) \propto \frac{\partial}{\partial z} G_0(p,z)$, we obtain a nonanalyticity $\propto z^{3/2}$. Note that uneven occurrences of $\mathbf{p}$ and/or $\mathbf{q}$, such as an isolated product $\mathbf{pq}$, are not rotation invariant and therefore do not contribute to the integral.

q is small: Now the second bracket delivers an additional nonanalyticity [19] q^2, which again produces a $z^{3/2}$ nonanalyticity.

We therefore conclude for this group of diagrams

$$\lim_{z\to 0} \lim_{k\to 0} \mathrm{Im}\left[\,\Sigma_\alpha^{(2)}(k,z)\,\right] \propto z^{3/2} k^2 \tag{15}$$

4.2. $\Sigma_\beta^{(2)}(k,z)$: *Irreducible Diagrams* $(1\,2\cdots 2\cdots 1)$

Since sites 1 and 2 are connected directly via t_{12}^o or t_{12}^d, the diagrams contain only three t's and two G_0's. Therefore, only eight diagrams are possible (cf. Figure 3):

$$\mathbf{OOO} = \rho \int d\mathbf{p}\, d\mathbf{q}\; t^2(p)\; t(q)\; G_0(p)\; G_0(q)$$

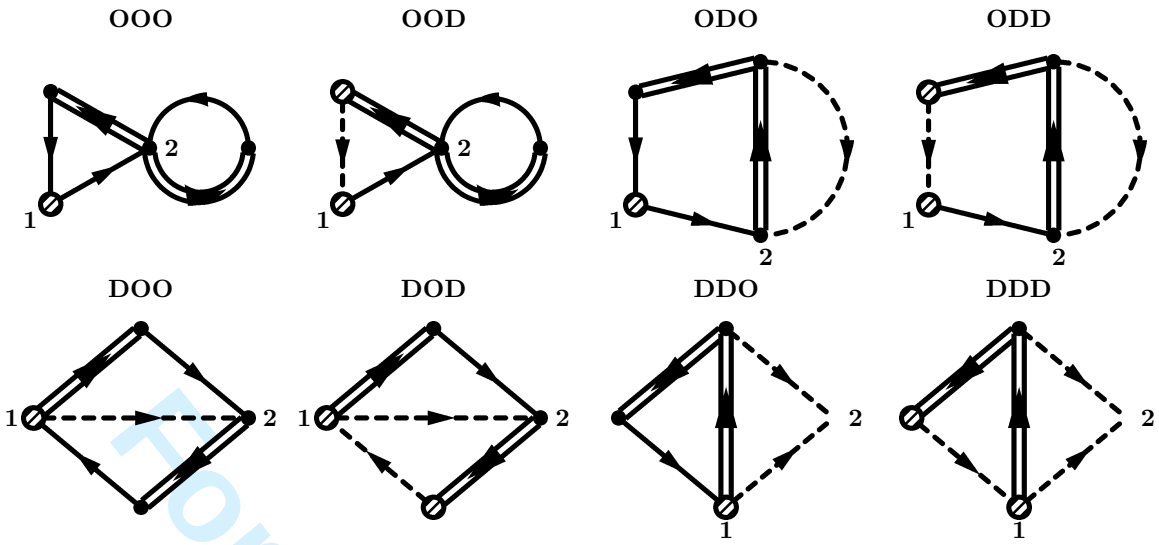

Figure 3. Irreducible Diagrams in $\Sigma_{\beta}^{(2)}(k,z)$

$$\mathbf{OOD} = -\rho \int d\mathbf{p}\, d\mathbf{q}\; t(\mathbf{k}-\mathbf{p})\; t(p)\; t(q)\; G_0(p)\; G_0(q)$$

$$\mathbf{ODO} = -\rho \int d\mathbf{p}\, d\mathbf{q}\; t^2(p)\; t(\mathbf{p}-\mathbf{q})\; G_0(p)\; G_0(q)$$

$$\mathbf{ODD} = \rho \int d\mathbf{p}\, d\mathbf{q}\; t(\mathbf{k}-\mathbf{p})\; t(p)\; t(\mathbf{p}-\mathbf{q})\; G_0(p)\; G_0(q)$$

$$\mathbf{DOO} = -\rho \int d\mathbf{p}\, d\mathbf{q}\; t(p)\; t(\mathbf{p}-\mathbf{q})\; t(q)\; G_0(p)\; G_0(q)$$

$$\mathbf{DOD} = \rho \int d\mathbf{p}\, d\mathbf{q}\; t(\mathbf{k}-\mathbf{p})\; t(\mathbf{p}-\mathbf{q})\; t(q)\; G_0(p)\; G_0(q)$$

$$\mathbf{DDO} = \rho \int d\mathbf{p}\, d\mathbf{q}\; t(p)\; t^2(\mathbf{p}-\mathbf{q})\; G_0(p)\; G_0(q)$$

$$\mathbf{DDD} = -\rho \int d\mathbf{p}\, d\mathbf{q}\; t(\mathbf{k}-\mathbf{p})\; t^2(\mathbf{p}-\mathbf{q})\; G_0(p)\; G_0(q)$$

Added together:

$$\Sigma_{\beta}^{(2)}(k,z) = \tag{16}$$
$$-\rho \int d\mathbf{p}\, d\mathbf{q}\, [t(\mathbf{k}-\mathbf{p}) - t(p)]\, [t(\mathbf{p}-\mathbf{q}) - t(p)]\, [t(\mathbf{p}-\mathbf{q}) - t(q)]\, G_0(p)\, G_0(q)$$

Because of (10), the first bracket gives us only a k^2. Depending on whether p or q are small, the third, respectively second, bracket delivers the required additional p^2, respectively q^2, to obtain:

$$\lim_{z\to 0} \lim_{k\to 0} \mathrm{Im}\left[\Sigma_{\beta}^{(2)}(k,z)\right] \propto z^{3/2}k^2 \tag{17}$$

Note a particular property of diagrams **DDO** and **DDD**:

If the propagator in the middle of the diagram collapses to the diagonal $\mathcal{G}_0$, as explained above, these diagrams are factorizable at site 1 and therefore not irreducible anymore. To avoid double counting, the diagonal term $\mathcal{G}_0$ must therefore be subtracted from this propagator.

It can be easily verified, however, that the $z^{3/2}$–nonanalyticity is not affected by this.

4.3. $\boldsymbol{\Sigma_{\gamma}^{(2)}(k,z)}$: *Irreducible Diagrams* $\mathbf{(1*2\cdots 1\cdots 2)}$

The crossover topology of these 16 diagrams (Figure 4) leads to more intricate convolution integrals.

Based on the following abbreviations

$$\begin{array}{rl} \boldsymbol{\alpha} := & \mathbf{k}-\mathbf{p}-\mathbf{q} \\ \boldsymbol{\beta} := & \mathbf{p} \\ \boldsymbol{\gamma} := & \mathbf{q} \\ \mathbf{a} := & \mathbf{p}+\mathbf{q} \\ \mathbf{b} := & \mathbf{k}-\mathbf{p} \\ \mathbf{c} := & \mathbf{k}-\mathbf{q} \end{array} \tag{18}$$

we obtain

$$\mathbf{OOOO} = \rho^2 \int\int d\boldsymbol{\beta}\, d\boldsymbol{\gamma} \quad G_0(\boldsymbol{\alpha})\, G_0(\boldsymbol{\beta})\, G_0(\boldsymbol{\gamma}) \cdot t(\boldsymbol{\alpha})\, t(\boldsymbol{\beta})\, t^2(\boldsymbol{\gamma})$$

$$\mathbf{OOOD} = -\rho^2 \int\int d\boldsymbol{\beta}\, d\boldsymbol{\gamma} \quad G_0(\boldsymbol{\alpha})\, G_0(\boldsymbol{\beta})\, G_0(\boldsymbol{\gamma}) \cdot t(\mathbf{a})\, t(\boldsymbol{\beta})\, t^2(\boldsymbol{\gamma})$$

$$\mathbf{OODO} = -\rho^2 \int\int d\boldsymbol{\beta}\, d\boldsymbol{\gamma} \quad G_0(\boldsymbol{\alpha})\, G_0(\boldsymbol{\beta})\, G_0(\boldsymbol{\gamma}) \cdot t^2(\boldsymbol{\alpha})\, t(\mathbf{a})\, t(\boldsymbol{\gamma})$$

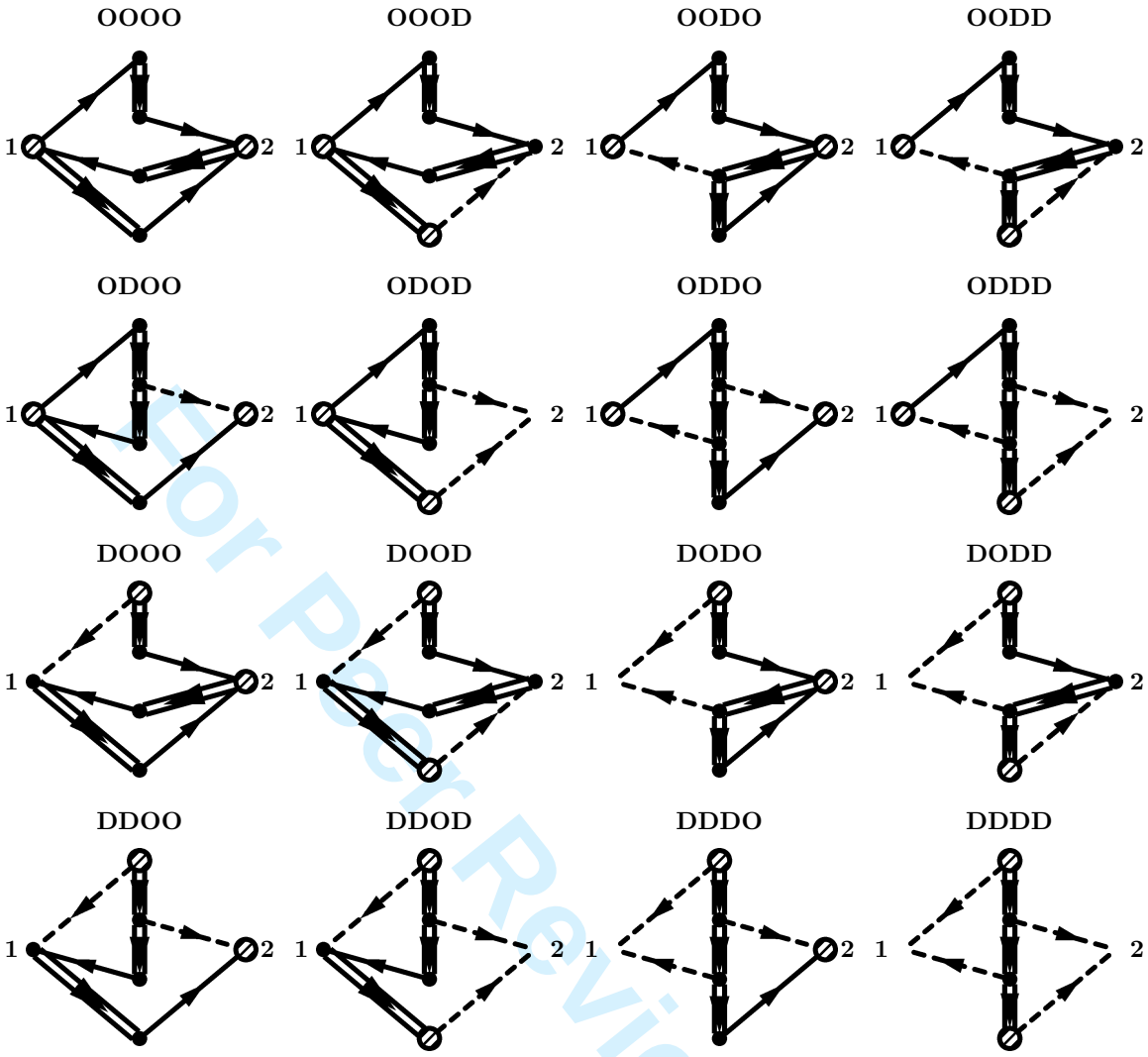

Figure 4. Irreducible Diagrams in $\Sigma_{\gamma}^{(2)}(k,z)$

$$\mathbf{OODD} = \rho^2 \int\int d\boldsymbol{\beta}\, d\boldsymbol{\gamma} \quad G_0(\boldsymbol{\alpha})\, G_0(\boldsymbol{\beta})\, G_0(\boldsymbol{\gamma}) \cdot t(\mathbf{b})\, t(\mathbf{c})\, t^2(\boldsymbol{\beta})$$

$$\mathbf{ODOO} = -\rho^2 \int\int d\boldsymbol{\beta}\, d\boldsymbol{\gamma} \quad G_0(\boldsymbol{\alpha})\, G_0(\boldsymbol{\beta})\, G_0(\boldsymbol{\gamma}) \cdot t(\boldsymbol{\alpha})\, t(\mathbf{a})\, t(\boldsymbol{\beta})\, t(\boldsymbol{\gamma})$$

$$\mathbf{ODOD} = \rho^2 \int\int d\boldsymbol{\beta}\, d\boldsymbol{\gamma} \quad G_0(\boldsymbol{\alpha})\, G_0(\boldsymbol{\beta})\, G_0(\boldsymbol{\gamma}) \cdot t^2(\mathbf{a})\, t(\boldsymbol{\beta})\, t(\boldsymbol{\gamma})$$

$$\mathbf{ODDO} = \rho^2 \int\int d\boldsymbol{\beta}\, d\boldsymbol{\gamma} \quad G_0(\boldsymbol{\alpha})\, G_0(\boldsymbol{\beta})\, G_0(\boldsymbol{\gamma}) \cdot t(\mathbf{b})\, t(\mathbf{c})\, t(\boldsymbol{\beta})\, t(\boldsymbol{\gamma})$$

$$\mathbf{ODDD} = -\rho^2 \int\int d\boldsymbol{\beta}\, d\boldsymbol{\gamma} \quad G_0(\boldsymbol{\alpha})\, G_0(\boldsymbol{\beta})\, G_0(\boldsymbol{\gamma})\, t(\mathbf{b})\, t^2(\mathbf{c})\, t(\boldsymbol{\beta})$$

$$\mathbf{DOOO} = -\rho^2 \int\int d\boldsymbol{\beta}\, d\boldsymbol{\gamma} \quad G_0(\boldsymbol{\alpha})\, G_0(\boldsymbol{\beta})\, G_0(\boldsymbol{\gamma}) \cdot t(\boldsymbol{\alpha})\, t(\mathbf{a})\, t(\boldsymbol{\beta})\, t(\boldsymbol{\gamma})$$

$$\mathbf{DOOD} = \rho^2 \int\int d\boldsymbol{\beta}\, d\boldsymbol{\gamma} \quad G_0(\boldsymbol{\alpha})\, G_0(\boldsymbol{\beta})\, G_0(\boldsymbol{\gamma}) \cdot t(\boldsymbol{\alpha})\, t(\mathbf{b})\, t(\mathbf{c})\, t(\boldsymbol{\beta})$$

$$\mathbf{DODO} = \rho^2 \int\int d\boldsymbol{\beta}\, d\boldsymbol{\gamma} \quad G_0(\boldsymbol{\alpha})\, G_0(\boldsymbol{\beta})\, G_0(\boldsymbol{\gamma}) \cdot t(\boldsymbol{\alpha})\, t^2(\mathbf{a})\, t(\boldsymbol{\gamma})$$

$$\mathbf{DODD} = -\rho^2 \int\int d\boldsymbol{\beta}\, d\boldsymbol{\gamma} \quad G_0(\boldsymbol{\alpha})\, G_0(\boldsymbol{\beta})\, G_0(\boldsymbol{\gamma}) \cdot t^2(\mathbf{b})\, t(\mathbf{c})\, t(\boldsymbol{\beta})$$

$$\mathbf{DDOO} = \rho^2 \int\int d\boldsymbol{\beta}\, d\boldsymbol{\gamma} \quad G_0(\boldsymbol{\alpha})\, G_0(\boldsymbol{\beta})\, G_0(\boldsymbol{\gamma}) \cdot t(\boldsymbol{\alpha})\, t(\mathbf{b})\, t(\mathbf{c})\, t(\boldsymbol{\gamma})$$

$$\mathbf{DDOD} = -\rho^2 \int\int d\boldsymbol{\beta}\, d\boldsymbol{\gamma} \quad G_0(\boldsymbol{\alpha})\, G_0(\boldsymbol{\beta})\, G_0(\boldsymbol{\gamma}) \cdot t(\boldsymbol{\alpha})\, t(\mathbf{b})\, t^2(\mathbf{c})$$

$$\mathbf{DDDO} = -\rho^2 \int\int d\boldsymbol{\beta}\, d\boldsymbol{\gamma} \quad G_0(\boldsymbol{\alpha})\, G_0(\boldsymbol{\beta})\, G_0(\boldsymbol{\gamma}) \cdot t^2(\mathbf{b})\, t(\mathbf{c})\, t(\boldsymbol{\gamma})$$

$$\mathbf{DDDD} = \rho^2 \int\int d\boldsymbol{\beta}\, d\boldsymbol{\gamma} \quad G_0(\boldsymbol{\alpha})\, G_0(\boldsymbol{\beta})\, G_0(\boldsymbol{\gamma}) \cdot t^2(\mathbf{b})\, t^2(\mathbf{c})$$

Collecting Terms

To derive a usable expression for the sum of these 16 diagrams, we have to exploit the symmetries of the problem.

Transforming variables $\mathbf{p}$, $\mathbf{q} \to \widetilde{\mathbf{p}}$, $\widetilde{\mathbf{q}}$ allows to arbitrarily permute $\boldsymbol{\alpha}$, $\boldsymbol{\beta}$, $\boldsymbol{\gamma}$ under the boundary condition that $\mathbf{a}$, $\mathbf{b}$, $\mathbf{c}$ perform the same permutation, as indicated in the following table:

$$\begin{array}{c} \boldsymbol{\alpha}\ \boldsymbol{\beta}\ \boldsymbol{\gamma}\ \mathbf{a}\ \mathbf{b}\ \mathbf{c} \\ \boldsymbol{\alpha}\ \boldsymbol{\gamma}\ \boldsymbol{\beta}\ \mathbf{a}\ \mathbf{c}\ \mathbf{b} \\ \boldsymbol{\beta}\ \boldsymbol{\alpha}\ \boldsymbol{\gamma}\ \mathbf{b}\ \mathbf{a}\ \mathbf{c} \\ \boldsymbol{\beta}\ \boldsymbol{\gamma}\ \boldsymbol{\alpha}\ \mathbf{b}\ \mathbf{c}\ \mathbf{a} \\ \boldsymbol{\gamma}\ \boldsymbol{\alpha}\ \boldsymbol{\beta}\ \mathbf{c}\ \mathbf{a}\ \mathbf{b} \\ \boldsymbol{\gamma}\ \boldsymbol{\beta}\ \boldsymbol{\alpha}\ \mathbf{c}\ \mathbf{b}\ \mathbf{a} \end{array} \tag{19}$$

For example, the transformation

$$\widetilde{\mathbf{p}} := \mathbf{k} - \mathbf{p} - \mathbf{q} \qquad \text{und} \qquad \widetilde{\mathbf{q}} := \mathbf{p} \tag{20}$$

leads to

$$\mathbf{k} - \mathbf{p} - \mathbf{q} \to \widetilde{\mathbf{p}} \tag{21}$$
$$\mathbf{p} \to \widetilde{\mathbf{q}} \tag{22}$$
$$\mathbf{q} \to \mathbf{k} - \widetilde{\mathbf{p}} - \widetilde{\mathbf{q}} \tag{23}$$
$$\mathbf{p} + \mathbf{q} \to \mathbf{k} - \widetilde{\mathbf{p}} \tag{24}$$
$$\mathbf{k} - \mathbf{p} \to \mathbf{k} - \widetilde{\mathbf{q}} \tag{25}$$
$$\mathbf{k} - \mathbf{q} \to \widetilde{\mathbf{p}} + \widetilde{\mathbf{q}} \tag{26}$$

and thus the permutation $\boldsymbol{\alpha}\,\boldsymbol{\beta}\,\boldsymbol{\gamma}\,\mathbf{a}\,\mathbf{b}\,\mathbf{c} \to \boldsymbol{\beta}\,\boldsymbol{\gamma}\,\boldsymbol{\alpha}\,\mathbf{b}\,\mathbf{c}\,\mathbf{a}$.

The product $G_0\,(\boldsymbol{\alpha})\,G_0\,(\boldsymbol{\beta})\,G_0\,(\boldsymbol{\gamma})$ is invariant with respect to these permutations and because of

$$\int\int d\boldsymbol{\alpha}\,d\boldsymbol{\beta} = \int\int d\boldsymbol{\alpha}\,d\boldsymbol{\gamma} = \int\int d\boldsymbol{\beta}\,d\boldsymbol{\gamma} \tag{27}$$

the integration variables can be chosen freely. After suitably regrouping the t–factors, we obtain for the sum of all diagrams the expression

$$\begin{aligned} K &:= \mathbf{OOOO} + \cdots + \mathbf{DDDD} \\ &= \rho^2 \int\int d\boldsymbol{\beta}\,d\boldsymbol{\gamma} \quad G_0\,(\boldsymbol{\alpha})\,G_0\,(\boldsymbol{\beta})\,G_0\,(\boldsymbol{\gamma}) \quad \times \\ &\times\, [\,t\,(\boldsymbol{\beta}) - t\,(\mathbf{b})\,] \cdot [\,t\,(\boldsymbol{\gamma}) - t\,(\mathbf{c})\,] \cdot [\,t\,(\boldsymbol{\gamma}) - t\,(\boldsymbol{\beta})\,] \cdot [\,t\,(\boldsymbol{\alpha}) + t\,(\boldsymbol{\beta})\,] \end{aligned}$$

Since we integrate over two variables only, we have to eliminate one G_0–factor. To this end, we apply a partial fraction decomposition

$$\rho\,[\,t\,(\boldsymbol{\gamma}) - t\,(\boldsymbol{\beta})\,] \cdot G_0\,(\boldsymbol{\beta})\,G_0\,(\boldsymbol{\gamma}) = [\,G_0\,(\boldsymbol{\gamma}) - G_0\,(\boldsymbol{\beta})\,] \tag{28}$$

Some further permutations and regrouping lead to

$$\begin{aligned} K = \rho^2 \int\int d\boldsymbol{\beta}\,d\boldsymbol{\gamma} \quad & G_0\,(\boldsymbol{\beta})\,G_0\,(\boldsymbol{\gamma}) \quad \times \\ & \times\, [\,t\,(\boldsymbol{\alpha}) - t\,(\mathbf{a})\,] \cdot [\,t\,(\boldsymbol{\alpha}) - t\,(\boldsymbol{\gamma})\,] \cdot [\,t\,(\boldsymbol{\gamma}) - t\,(\mathbf{c})\,] \end{aligned}$$

After reinserting the above definitions, we can expand for small k:

$$t(\boldsymbol{\alpha}) - t(\mathbf{a}) = t(\mathbf{k} - \mathbf{p} - \mathbf{q}) - t(\mathbf{p} + \mathbf{q})$$
$$= \frac{t'(\mathbf{p} + \mathbf{q})}{|\mathbf{p} + \mathbf{q}|} \cdot \mathbf{k}(\mathbf{p} + \mathbf{q}) + \mathcal{O}(k^2)$$

$$t(\mathbf{c}) - t(\boldsymbol{\gamma}) = t(\mathbf{k} - \mathbf{q}) - t(q)$$
$$= \frac{t'(q)}{q} \cdot \mathbf{kq} + \mathcal{O}(k^2)$$

We thus obtain $\lim_{k \to 0} K \propto k^2$, as required. Since we only consider the lowest-order term, we may use

$$t(\boldsymbol{\alpha}) - t(\boldsymbol{\gamma}) = t(\mathbf{a}) - t(\boldsymbol{\gamma}) + \mathcal{O}(k) \tag{29}$$

and set

$$t(\boldsymbol{\alpha}) - t(\boldsymbol{\gamma}) \approx t(\mathbf{p} + \mathbf{q}) - t(q) \tag{30}$$

We thus finally arrive at

$$K = \rho^2 \int\int d\mathbf{p}\, d\mathbf{q} \quad G_0(\mathbf{p})\, G_0(\mathbf{q}) \quad \times \tag{31}$$
$$\times \underbrace{\left[\frac{t'(\mathbf{p} + \mathbf{q})}{|\mathbf{p} + \mathbf{q}|} \cdot \mathbf{k}(\mathbf{p} + \mathbf{q}) \right]}_{A} \cdot \underbrace{[\, t(\mathbf{p} + \mathbf{q}) - t(q)\,]}_{B} \cdot \underbrace{\left[\frac{t'(q)}{q} \cdot \mathbf{kq} \right]}_{C} + \mathcal{O}(k^3)$$

For the analytical properties, we again have to consider two cases:

q is small:

Bracket C gives us a factor q, but brackets A and B approach a finite value for $q \to 0$.

But: After setting $\mathbf{q} = \mathbf{0}$ in A and B, both the integral over $\mathbf{p}$ (because of the $\mathbf{kp}$ term in A) and over $\mathbf{q}$ (due to the $\mathbf{kq}$ in C) vanish due to lack of rotational invariance. Consequently, we have to expand the fraction in A to first order in q, which provides us with an additional factor $\mathbf{pq} \propto q$. Now rotational invariance is preserved and a $z^{3/2}$ nonanalyticity is obtained.

p is small:

Bracket C remains finite and B leads to a factor $\mathbf{pq} \propto p$.

Setting $\mathbf{p} = \mathbf{0}$ in A leads to the following structure

$$\int\int d\mathbf{p}\, d\mathbf{q} \quad f(q) \cdot [\, \mathbf{pq}\,] \cdot [\, \mathbf{kq}\,]^2 \tag{32}$$

In order to restore rotational invariance, we again have to expand in A to first order in p, which yields an additional $\mathbf{pq} \propto p$ and leads to a $z^{3/2}$ nonanalyticity.

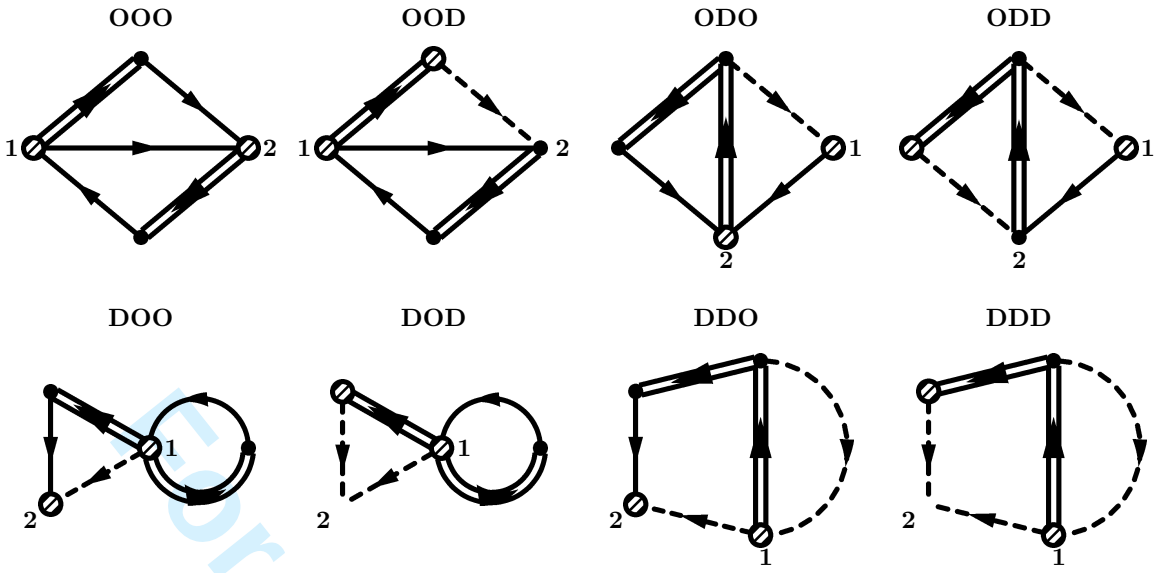

Figure 5. Irreducible Diagrams in $\Sigma_{\delta}^{(2)}(k,z)$

We thus conclude that

$$\lim_{z\to 0}\lim_{k\to 0}\mathrm{Im}\left[\Sigma_{\gamma}^{(2)}(k,z)\right]\propto z^{3/2}k^{2} \tag{33}$$

holds.

4.4. $\boldsymbol{\Sigma_{\delta}^{(2)}(k,z)}$: *Irreducible Diagrams* $(\mathbf{1\,2\cdots 1\cdots 2})$

Similar to Σ_{β} above, 8 diagrams need to be considered (Figure 5):

$$\mathbf{OOO}=\rho\int d\mathbf{p}\,d\mathbf{q}\;t\left(\mathbf{k}-\mathbf{p}+\mathbf{q}\right)\;t\left(p\right)\;t\left(q\right)\;G_{0}\left(p\right)\;G_{0}\left(q\right)$$

$$\mathbf{OOD}=-\rho\int d\mathbf{p}\,d\mathbf{q}\;t\left(\mathbf{k}-\mathbf{p}+\mathbf{q}\right)\;t\left(\mathbf{k}-\mathbf{p}\right)\;t\left(q\right)\;G_{0}\left(p\right)\;G_{0}\left(q\right)$$

$$\mathbf{ODO}=-\rho\int d\mathbf{p}\,d\mathbf{q}\;t\left(\mathbf{k}-\mathbf{p}+\mathbf{q}\right)\;t\left(p\right)\;t\left(\mathbf{p}-\mathbf{q}\right)\;G_{0}\left(p\right)\;G_{0}\left(q\right)$$

$$\mathbf{ODD}=\rho\int d\mathbf{p}\,d\mathbf{q}\;t\left(\mathbf{k}-\mathbf{p}+\mathbf{q}\right)\;t\left(\mathbf{k}-\mathbf{p}\right)\;t\left(\mathbf{p}-\mathbf{q}\right)\;G_{0}\left(p\right)\;G_{0}\left(q\right)$$

$$\mathbf{DOO}=-\rho\int d\mathbf{p}\,d\mathbf{q}\;t\left(\mathbf{k}-\mathbf{p}\right)\;t\left(p\right)\;t\left(q\right)\;G_{0}\left(p\right)\;G_{0}\left(q\right)$$

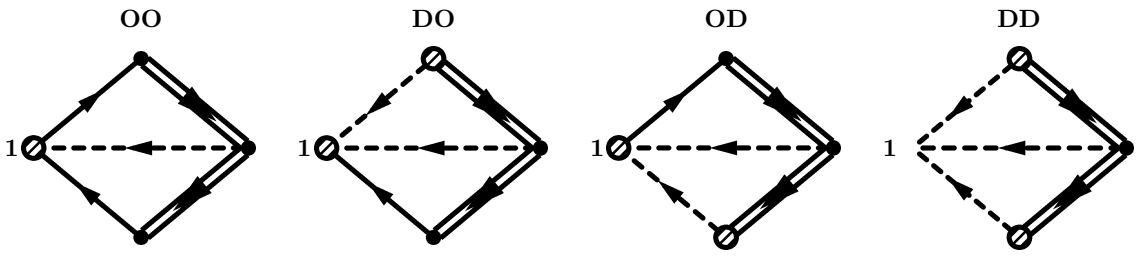

Figure 6. Irreducible Diagrams in $\Sigma_{\varepsilon}^{(2)}(k,z)$

$$\mathbf{DOD} = \rho \int d\mathbf{p}\, d\mathbf{q}\; t^2(\mathbf{k}-\mathbf{p})\; t(q)\; G_0(p)\; G_0(q)$$

$$\mathbf{DDO} = \rho \int d\mathbf{p}\, d\mathbf{q}\; t(\mathbf{k}-\mathbf{p})\; t(p)\; t(\mathbf{p}-\mathbf{q})\; G_0(p)\; G_0(q)$$

$$\mathbf{DDD} = -\rho \int d\mathbf{p}\, d\mathbf{q}\; t^2(\mathbf{k}-\mathbf{p})\; t(\mathbf{p}-\mathbf{q})\; G_0(p)\; G_0(q)$$

Added together:

$$\Sigma_{\delta}^{(2)}(k,z) \quad \propto \tag{34}$$
$$\rho \int d\mathbf{p}\, d\mathbf{q}\; [\,t(\mathbf{k}-\mathbf{p}) - t(p)\,]\,[\,t(\mathbf{k}-\mathbf{p}+\mathbf{q}) - t(\mathbf{k}-\mathbf{p})\,]\,[\,t(\mathbf{p}-\mathbf{q}) - t(q)\,]\; G_0(p)\; G_0(q)$$

The first bracket is proportional to k^2. Depending on whether p or q is small, the third or second bracket yields the required additional p^2 or q^2, respectively.

Thus we have here too:

$$\lim_{z\to 0}\lim_{k\to 0} \mathrm{Im}\left[\Sigma_{\delta}^{(2)}(k,z)\right] \propto z^{3/2}k^2 \tag{35}$$

4.5. $\boldsymbol{\Sigma_{\varepsilon}^{(2)}(k,z)}$: *Irreducible Diagrams* $(\mathbf{1}\cdots\mathbf{1}\cdots\mathbf{1})$

Here only 4 cases are possible (Figure 6).

$$\mathbf{OO} = -\rho \int d\mathbf{p}\, d\mathbf{q}\; t(p)\; t(\mathbf{p}-\mathbf{q})\; t(q)\; G_0(p)\; G_0(q)$$

$$\mathbf{OD} = \rho \int d\mathbf{p}\, d\mathbf{q}\; t(\mathbf{k}-\mathbf{p})\; t(\mathbf{p}-\mathbf{q})\; t(q)\; G_0(p)\; G_0(q)$$

$$\mathbf{DO} = \rho \int d\mathbf{p}\, d\mathbf{q}\; t\,(\mathbf{k}-\mathbf{q})\; t\,(p)\; t\,(\mathbf{p}-\mathbf{q})\; G_0\,(p)\; G_0\,(q)$$

$$\mathbf{DD} = -\rho \int d\mathbf{p}\, d\mathbf{q}\; t\,(\mathbf{k}-\mathbf{p})\; t\,(\mathbf{k}-\mathbf{q})\; t\,(\mathbf{p}-\mathbf{q})\; G_0\,(p)\; G_0\,(q)$$

Added together:

$$\Sigma_{\varepsilon}^{(2)}\,(k,z) \quad \propto \tag{36}$$
$$\rho \int d\mathbf{p}\, d\mathbf{q}\; [\,t\,(\mathbf{k}-\mathbf{p}) - t\,(p)\,]\,[\,t\,(\mathbf{k}-\mathbf{q}) - t\,(q)\,]\; t\,(\mathbf{p}-\mathbf{q})\; G_0\,(p)\; G_0\,(q)$$

For order $\mathcal{O}\left(k^2\right)$, because of (10), the first two brackets muts be proportional to $\propto \mathbf{kp}$ and $\mathbf{kq}$, respectively. For rotational invariance, the last bracket needs to be expanded and thus provides the additional required $\mathbf{pq}$ term, to obtain:

$$\lim_{z\to 0}\lim_{k\to 0} \mathrm{Im}\left[\,\Sigma_{\varepsilon}^{(2)}\,(k,z)\,\right] \propto z^{3/2}k^2 \tag{37}$$

With (13) it follows immediately

$$\lim_{z\to 0}\lim_{k\to 0} \mathrm{Im}\left[\,\Sigma^{(2)}\,(k,z)\,\right] \propto z^{3/2}k^2 \tag{38}$$

5. Conclusion

Working out term by term in the second-order self energy we have convinced ourselves that to this order the nonalytic behavior (38), which both leads to Rayleigh-type sound attenuation and to the correct long-time tail in the analogous diffusion problem is recovered. This is in contrast to the claims in the publications [7]. In these publications a self-consistent equation for the self-energy is advocated, which consists in making the first-order result (8) self-consistent, i.e. replacing the 0-th-order Green's function by the full one. Now, in performing a high-density expansion of this equation one easily convinces oneself that the corresponding diagrams are

- the entire sum $\Sigma_{\alpha}^{(2)}(k,z)$;
- the diagrams **OOO**, **OOD**, **ODO**, **ODD** of $\Sigma_{\beta}^{(2)}(k,z)$, but not the remaining four diagrams;
- the diagrams **DOO**, **DOD**, **DDO**, **DDD** of $\Sigma_{\delta}^{(2)}(k,z)$, but not the remaining four diagrams.

As the partial sums do not give the correct analytic properties, this is the reason, why the self-consistent scheme advocated by [7] does not lead to Rayleigh scattering. We shall publish shortly a self-consistent scheme, which includes Rayleigh scattering.

References

[1] J. W. Strutt, Third Baron Rayleigh, Philos. Mag. **41**, 247 and 447 (1871); **47**, 375 (1899); repr. in *Lord Rayleigh, Scientific Papers* **1**, 87 and 104 (1899); **4**, 397 (1903). Cambridge Univ. Press 1899-1920
[2] E. Akkermans, R. Maynard, Phys. Rev. B **32**, 7850 (1985).
[3] B. Ruffle et al., PRL. 96, 045502 (2006)
[4] G. Monaco, V. M. Giordano, PNAS 106, 3659 (2009)
[5] G. Baldi et al., PRL 104, 195501 (2010)
[6] C. Ganter, W. Schirmacher, Phys Rev B, in press
[7] V. Martín-Mayor *et al.* J. Chem. Phys. **114**, 8068 (2001); T. S. Grigera *et al.* Phys. Rev. Lett. **87**, 085502 (2001); T. S. Grigera *et al.* J. Phys. Condens. Matter **14**, 2167 (2002) S. Ciliberti *et al.*, J. Chem. Phys. **119**, 8577 (2003); T. S. Grigera *et al.*, Nature (London) **422**, 289 (2003).
[8] A. Miller, E. Abrahams, Phys. Rev. **120**, 745 (1960).
[9] V. Ambegaokar, B. I. Halperin, J. S. Langer, Phys. Rev. B **4**, 2612 (1971).
[10] J. Haus *et al.*, Z. Phys. B **50**, 161 (1983).
[11] B. L. Shklovskii, A. L. Efros, *Electroic Properties of Doped Semiconductors*, Springer, Berlin, 1984
[12] H. Böttger, V. V. Bryksin, *Hopping Conduction in Solids*, Akademie-Verlag Berlin 1985
[13] M. H. Ernst *et al.*, J. statistical Phys. **34**, 477 (1984); J. Machta *et al.*, *ibid.*, **35**, 413 (1984).
[14] M. H. Ernst, A. Weyland, Phys. Lett. **34A**, 39 (1971).
[15] F. Höfling *et al.*, Phys. Rev. Lett. **96**, 165901 (2006)
[16] W. Feller, *An Introduction to Probability Theory and Its Applications*, Wiley, NY, 1950
[17] The real-space transition rate will always carry the letter r in the argument. In all other occations, it will refer to the Fourier transform.
[18] For better readability, the z–dependence of G_0 will be suppressed in the following.
[19] In the following we shall not explicitly mention the q^2 from the integration.

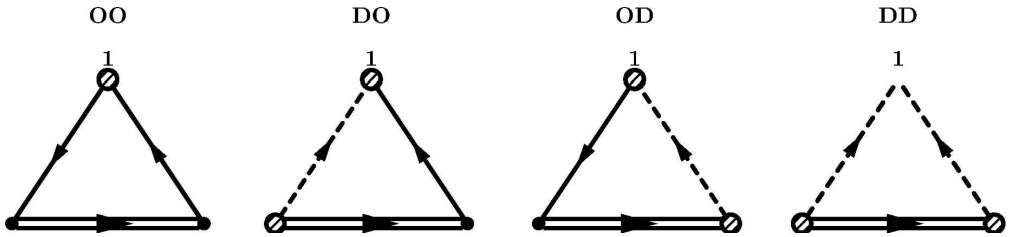

Irreducible diagrams in $\Sigma^{(1)}(k,z)$.

Off-diagonal matrix elements, $t^{o}_{ij} \equiv t(r_{ij})$,
associated with a site change, are represented by solid lines.
Dashed lines do not effect a site change. The associated transition
rates $t^{d}_{ij} \equiv - t(r_{ij})$ belong to the diagonal matrix
elements and are a consequence of the sum rule.

The unrenormalized propagator $[G_0]_{ij} \equiv$
$G_0(r_{ij})$ is shown as a double-line.
Note that the propagator contains a diagonal part (for i = j the diagram has
length zero)
$G_0(z) := [z + \rho t(0)]^{-1}$,
which is
formally obtained as G0(z) =
$\lim_{k\to\infty} G_0(k,z)$. In most cases, this requires no
special attention. Exceptions, when these terms need to be explicitly excluded
to preserve irreducibility will be mentioned below.

Open circles will always indicate start and end points of a diagram.
156x35mm (600 x 600 DPI)

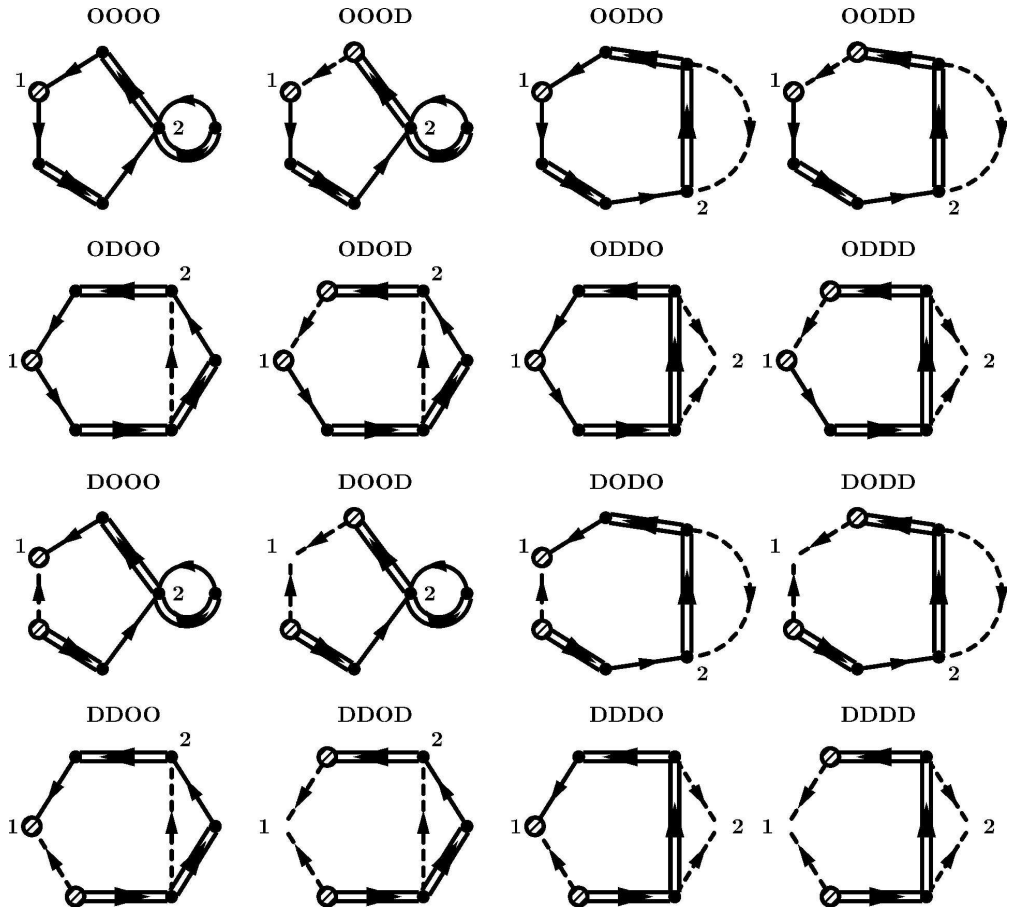

Irreducible Diagrams in $\Sigma_\alpha^{(2)}(k,z)$
163x146mm (600 x 600 DPI)

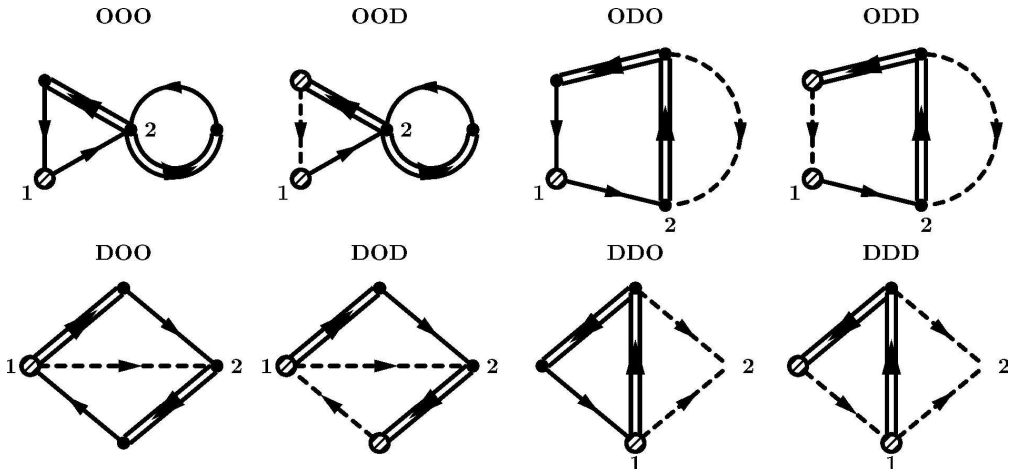

Irreducible Diagrams in $\Sigma_{\beta}^{(2)}(k,z)$
161x74mm (600 x 600 DPI)

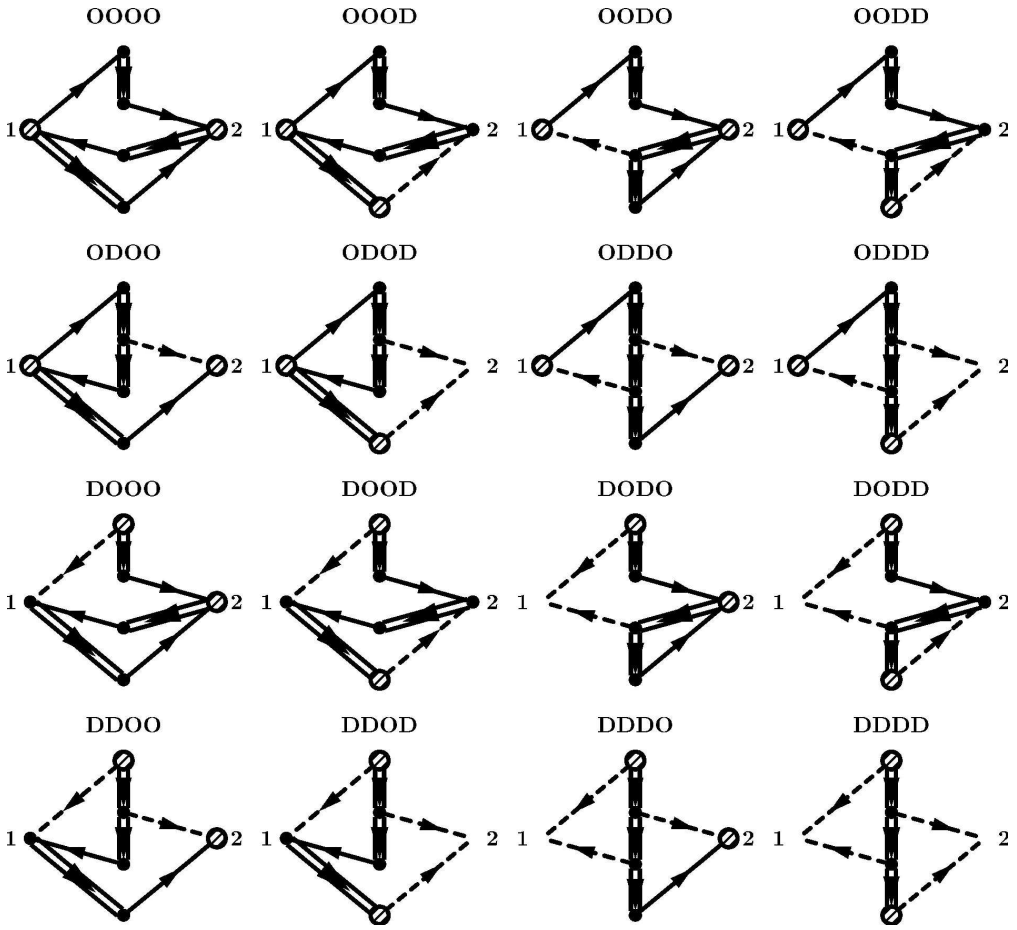

Irreducible Diagrams in $\Sigma_v^{(2)}(k,z)$
161x147mm (600 x 600 DPI)

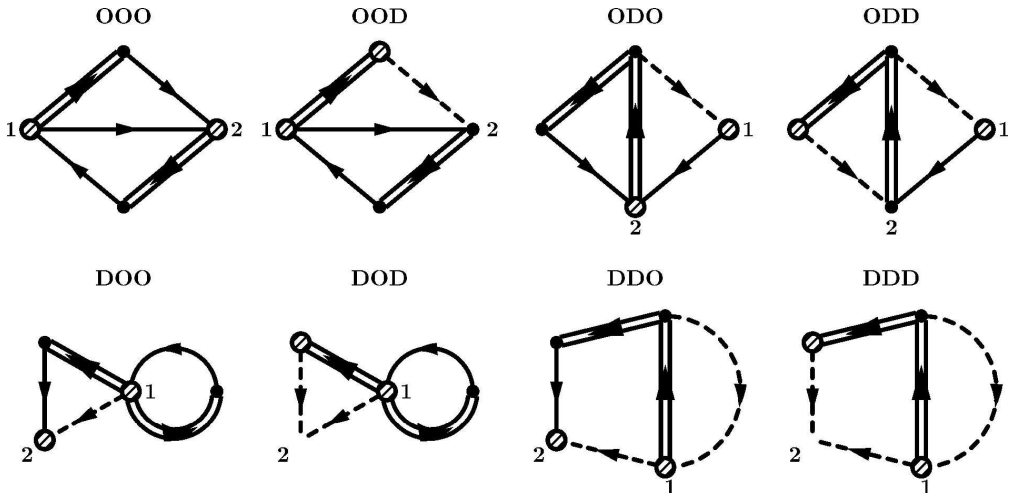

Irreducible Diagrams in $\Sigma_{\delta}^{(2)}(k,z)$
161x77mm (600 x 600 DPI)

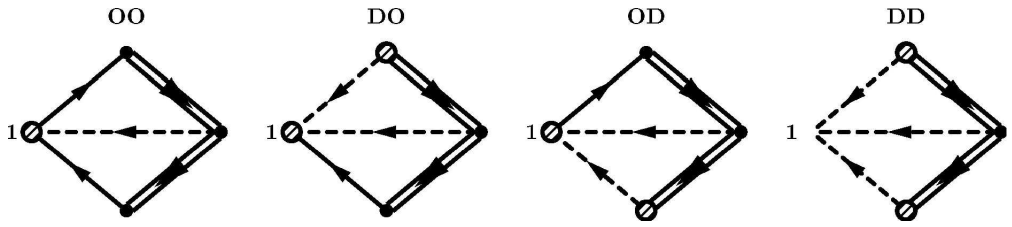

Irreducible Diagrams in $\Sigma_{\varepsilon}^{(2)}(k,z)$
158x33mm (600 x 600 DPI)